MANSOURA JOURNAL OF CHEMISTRY
Official Journal of Faculty of Science, Mansoura University, Egypt
E-mail: scimag@mans.edu.eg ISSN: 2974-4938

Fabrication AND INVESTIGATION OF BICHALCOPHENES-LOADED POLYMERS

Maha M. Abdelhamid, Mohamed A. Ismail and Magdy Y. Abdelaal*

Chemistry Department, Faculty of Science, Mansoura University, ET-35516-Mansoura, Egypt

**** Corresponding author** (MY. Abdelaal: myabdelaal@gmail.com & abdelaal@mans.edu.eg)*

Received:1/4/2021
Accepted: 6/4/2021

Abstract: Controlled release formations of drugs were prepared from bichalcophene derivatives as drugs and sodium carboxymethylcellulose (NaCMC) as a matrix of natural polysaccharide. The release behavior of bichalcophene derivatives from the NaCMC matrix was studied. The solubility and chemical nature of these derivatives have a significant effect on their release characteristics. The current study showed that the cationic amidinic bichalcophene derivatives exhibit a slow release rate due to the formation of hydrogen bonds between their positively charged amino groups and the negatively charged carboxyl groups of the polymer matrix. The derivatives of poor solubility exhibit a slow release rate while soluble derivatives show a fast release rate.

keywords: Bichalcophenes, Amidines, CMC, controlled release

1.Introduction

Carbohydrate polymers are extensively used in recent years in biomedical and pharmaceutical applications due to their biocompatibility and biodegradability [1-6]. However, the use of natural carbohydrate polymers like polysaccharides and proteins for biomedical, environmental, and analytical applications has attracted the attention of many investigators [7-15]. Carboxymethylcellulose (CMC) is the most common cellulose type among cellulose ethers. CMC is used in the food industry and production of non-food materials such as cement, ceramics, adhesives, textiles, paper, biocides, detergents, cosmetics, and pharmaceuticals as water-soluble cellulose derivatives. Preparation of CMC occurs by Williamson ether synthesis from alkali cellulose with monochloroacetic acid or its sodium salt in an aqueous-alcoholic medium. The manufacture of CMC is accomplished in two steps. The first step involves a suspension of cellulose in an alkali resulting in opening the bound cellulose chains and water penetration while the second step involves the reaction of cellulose with sodium monochloroacetate forming sodium carboxymethylcellulose. On the other hand, bichalcophenes have significant use in solvatochromic, photosensitizing, and photovoltaic cell applications [16-18]. Chalcophene-based compounds are important synthetic precursors for biologically active materials. α-Terthienyl **I** (**Fig. 1**) is a natural product and considered an antiviral, anti-infective, and photosensitizing agent [19,20]. Aryl-2,2'-bichalcophene derivatives of formula **II** (Fig. 1) have been reported for their antimicrobial [21,22], antimutagenic [23], and anticancer [24] activities. The current study focuses on the utilization of CMC as a carrier for the amidinic bichalcophenes to be released in an aqueous medium where the rate of release of the bichalcophene compounds from the CMC matrix has been investigated.

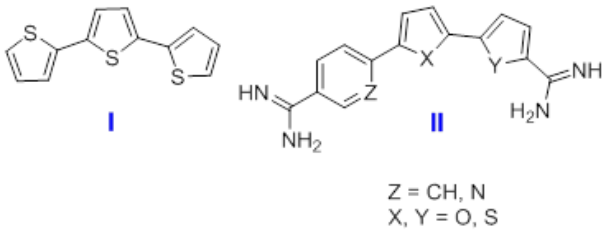

Fig. 1: Biologically important thiophenes

2. Materials and Methods

2.1. Materials and instruments

CMC (MW 41 kDa) was purchased from Alpha Chemika, India. The bichalcophenes (**Fig. 2**) were prepared as described previously [21]. All other chemicals and solvents were purchased from Sigma Aldrich unless otherwise mentioned. FT-IR spectra (KBr) were explored on Thermo Scientific Nicolet iS10 FT-IR Spectrometer. UV/Vis absorption spectra were

measured in the region of 200–600 nm on a Shimadzu 1700 Spectrometer while the thermogravimetric analysis (TGA) was achieved on Shimadzu TGA-50H in N_2 atmosphere and at a heating rate of 1°C/min.

2.2. Preparation of bichalcophenes-blended CMC films: General Procedure

Dissolve 0.5 g of sodium carboxymethyl-cellulose (**NaCMC**) in 50 mL distilled water with stirring for 2 h, and then add to a solution of a certain amount of each compound of the investigated bichalcophenes in 10 mL distilled water while stirring. The mixture was stirred for 2 h further, then poured into a Petri dish to form a thin film and left for dryness in an Oven at 60°C for 48 h. The formed blended film was then removed from the Petri dish and kept until use. The blended films were subjected to FT-IR spectroscopic analysis and the thermal weight loss percentage of CMC blends was determined through TGA analysis. The used amounts of the bichalcophenes are 40 mg of **1F** & **1S**, 30 mg of **2F**, and 16 mg of **3F** considering that **F** and **S** denote Free-base and Salt forms, respectively.

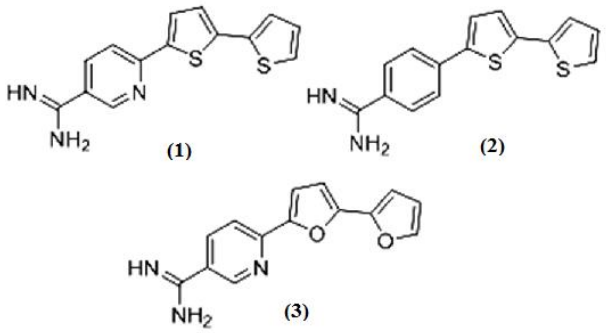

Fig. 2: The investigated bichalcophene derivatives for controlled release

2.3. Drug Release Study on CMC blends

A drug release study was performed using 50 mL of deionized water as a dissolution medium. Aliquots of 1 mL of the released medium were collected at 5, 15, 30, 60, 120, 240, 1440, 1500, 1560, and 1680 min where the release medium was replenished with an equal volume of dissolution medium. The absorbance of the release samples was measured using UV/Vis Spectrometer at λ_{max} of 426, 452, 428, and 428nm for **1F**, **2F**, **2S,** and **3F**, respectively. Time dependence of the released amount of bichalcophenes was plotted for each derivative.

3. Results and Discussion

3.1. FT-IR Spectroscopy of CMC blends

3.1.1. For CMC-1S blend

The interaction between the components of the blend provides valuable information at the molecular level. FT-IR spectra of CMC-**1S** (**Fig. 3**) showed the characteristic bands of the –OH group stretching for CMC at 3420 cm^{-1}, C-H stretching at 2924 cm^{-1} for $–CH_2$ and $–CH_3$ groups existing in the polymer backbone, at 1623 cm^{-1} for carbonyl vibration of carboxylate anion ($–COO^-$) and C=N, C=C stretch of the drug molecule, at 1428 cm^{-1} for C-H bending of $–CH_2$ and $–CH_3$ groups in the polymer, and at 1139 cm^{-1} & 1056 cm^{-1} for C-O stretching in the ester carboxylate anion [25].

3.1.2. For CMC-1F blend

Comparison of FT-IR spectrum of CMC-**1F** with that of CMC-**1S** showed the characteristic bands of –OH stretching of CMC-**1F** at 3439 cm^{-1} with a shift up relative to that of CMC-**1S** at 3420 cm^{-1} as shown in **Fig. 3**. This may be attributed to the weak H-bonding between CMC–OH groups and water molecules in the case of the salt blend. On the other hand, stronger hydrogen bonding may be formed in the case of CMC-**1F** blend between CMC–OH groups and N- atom of pyridine ring and/or amino group of **1F** considering that such hydrogen bonding may be weaker than that of water molecules due to their smaller size. Other absorption bands were shown at 2923 cm^{-1} of C-H stretching of $–CH_2$ and $–CH_3$ groups in CMC backbone, at 1606 cm^{-1} for C=O vibration in COO^-. Such absorptions are also shifted down to lower "ν" in case of **1F** blend relative to that for **1S** blend. This may be explained by the possible H-bonding between C=O groups of CMC and the free amino group of **1F**. Absorption was also observed at 1417 cm^{-1} related to C-H bending of $–CH_2$ and $–CH_3$ in CMC beside the absorptions at 1120 cm^{-1} and 1200 cm^{-1} of C-O- stretching for COO^- groups.

3.1.3. For CMC-2F and CMC-3F blends

Comparison of the FT-IR spectra of both CMC-**2F** and CMC-**3F** in Fig. 4 shows the characteristic bands of –OH stretching of CMC at 3441 cm^{-1} and 3559 cm^{-1} with a shift to the right in the case of CMC-**2F**. This may be

attributed to the formation of strong additional hydrogen bonding between hydroxyl groups of CMC and amino groups of **2F**. C-H stretching of $–CH_2$ and $–CH_3$ groups appears at 2923 cm^{-1}. The absorptions appear at 1741 cm^{-1} for the ester carbonyl group in CMC-**2F**, at 1666, 1644 cm^{-1} for C=N and/or C=C stretch of the drug molecule, at 1616 cm^{-1} and 1603 cm^{-1} for C=O group vibration for carboxylate anion with a shift to right in case of CMC-**3F**. This may be attributed to the tendency of C=O group of COO^- to form hydrogen bonds with the amino groups of **3F** [25].

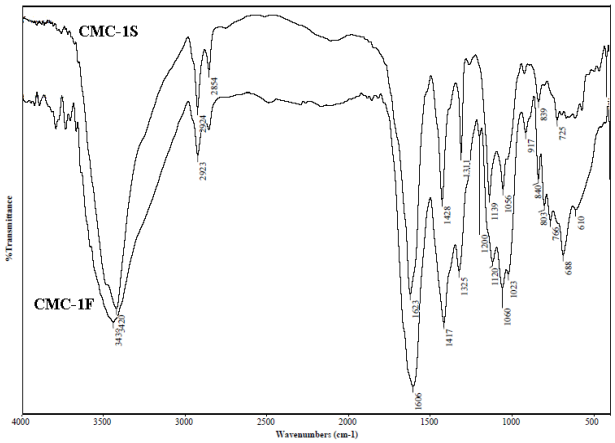

Fig. 3: FT-IR Spectra of CMC-**1F** and CMC-**1S** blends

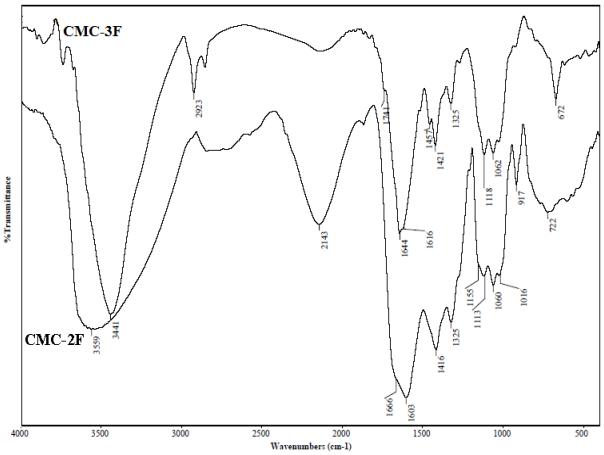

Fig. 4: FT-IR spectra of CMC-**2F** and CMC-**3F** blends

3.2. TGA Characterization of CMC blends:

3.2.1. For CMC-1S and CMC-1F blends Fig. 5 shows TGA analysis of CMC-**1S** blend which was degraded in three stages, at 47°C with weight loss of 23%, at 265°C with weight loss of 20%, and at 588°C with weight loss of 7%. These results indicate that the addition of bichalcophene salt facilitates the weight loss of CMC-**1S** and its stability is reduced under the thermal effect reflecting the weakness of the bond between CMC and **1S**.

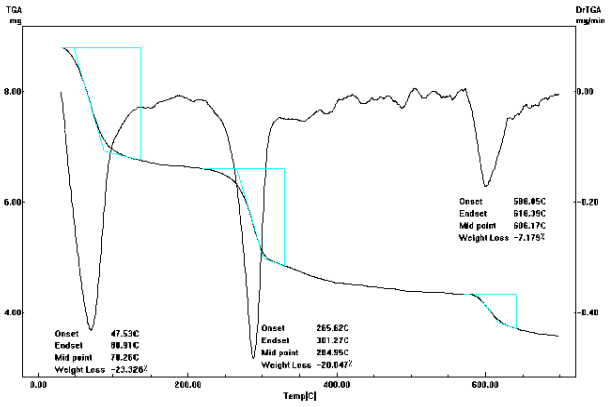

Fig. 5: TGA analysis (TGA) of CMC-**1S** blends

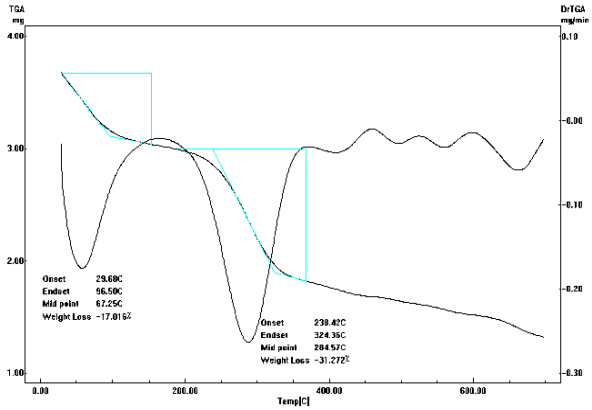

Fig. 6: TGA analysis (TGA) of CMC-**1F** blends

It is obvious from Fig. 6 that the degradation of CMC-**1F** differs from that of CMC-**1S** where it degrades in two stages at 29°C and 250°C with weight loss of 14% and 22%, respectively indicating that the addition of **1F** to CMC triggers its degradation. This may be attributed to the weak hydrogen bonding between –OH groups and C=O group of COO^- anion of CMC and the free amino groups of **1F** replacing partly the strong hydrogen bonding between OH groups on different CMC chains.

3.2.2. For CMC-2F and CMC-3F blends

TGA analysis for CMC-**2F** and CMC-**3F** are almost similar where the degradation for CMC-**2F** occurs through three stages at 33.96°C, 262°C and 596°C with weight loss of 17%, 18%, and 8%, respectively. The degradation stages for CMC-**3F** were observed at 33.15°C, 264°C and 537°C with weight loss of 13%, 24%, and 3%, respectively as shown in Fig. 7. These results indicate the relative higher stability of CMC-**2F** and CMC-**3F** compared to CMC-**1F**. This may be attributed to the relative strength of hydrogen bonding between CMC

and each of **2** and **3** compared to that with **1F**, while the results of weight loss indicate the weakness of intermolecular H-bonding between CMC and bichalcophene derivatives compared to the intramolecular hydrogen bonding within CMC matrix. Fig. 8 shows TGA analysis of CMC-**3F**.

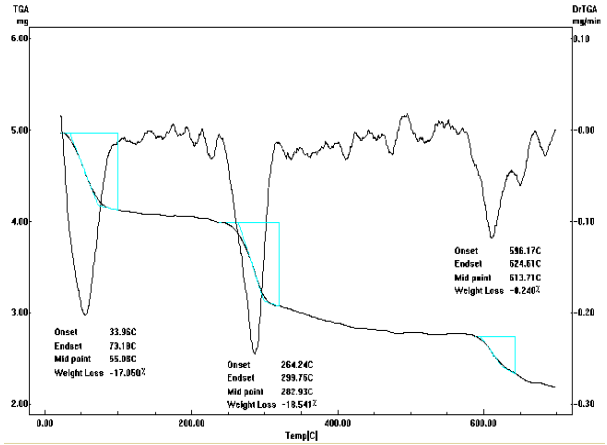

Fig. 7: TGA analysis (TGA) of CMC-**1F** blends

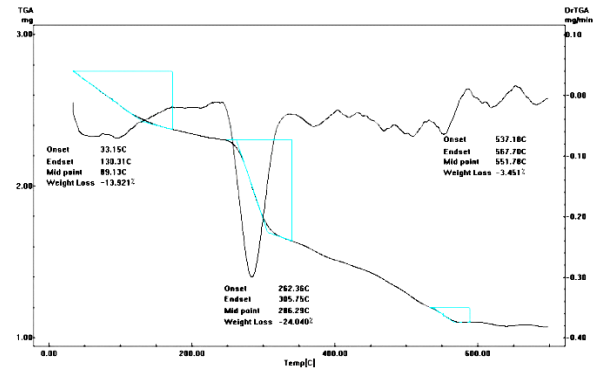

Fig. 8: TGA analysis (TGA) of CMC-**3F** blends

3.3. Drug Release Study of CMC blends

3.3.1. For CMC-1S blend

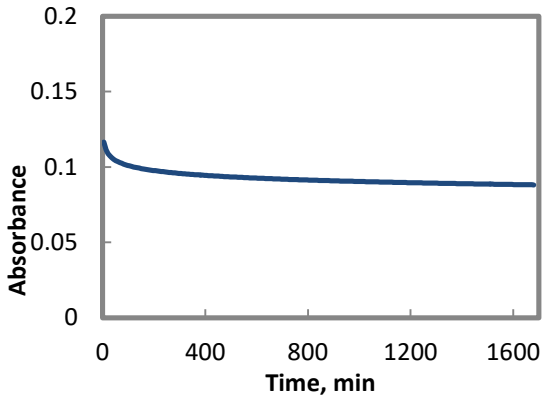

Fig. 9: Release of **1S** from CMC-**1S** blend under the room temperature and neutral pH

Fig. 9 shows the release of **1S** with time from CMC-**1S** indicating high initial amount of release, which may be attributed to the hydration of surface layers of the film leading to a quick release of the surface portion of compound **1S** along with the less bounded molecules of **1S** to the CMC matrix. By the time, the CMC blend showed a gradual decrease in the release of **1S** from the CMC matrix which may be attributed to the slow diffusion of water molecules into the CMC matrix due to the poor solubility of **1S** in the releasing media along with the strong hydrogen bonding formed between **1S** and OH groups on different chains of CMC. After that, the high swelling ability of CMC leads to the formation of highly swollen gel with increasing viscosity and hence retarding the release of **1S** from the CMC matrix. On the other hand, further slow release of **1S** from the CMC matrix continues which may be attributed to the transformation of CMC from the salt form into the relatively less soluble acid form through the ionic interaction between the carboxylate anion functionality (COO^-) in CMC and the positively charged amino group of **1S**. Such relatively low solubility of the acid form of CMC in water causes retardation of the release process of **1S** from the matrix. After a long time up to 28 h, another increase in the release was observed which may be attributed to the disintegration of the physical interactions linking the polymer chains due to the long contact of the film with the dissolution medium with the help of the hydrolytic pressure of water inside the matrix [26-29].

3.3.2. For CMC-1F blend

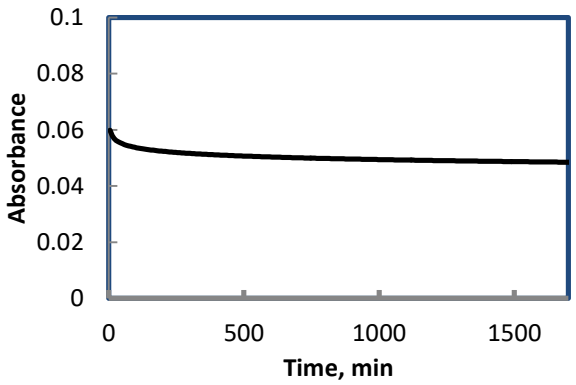

Fig. 10: Release of **1F** from CMC-**1F** blend at room temperature and neutral pH

Fig. 10 shows the release dependence of **1F** from its blend with CMC. The increase in **1F** release may be attributed to erosion or hydration of CMC surface first resulting in the

release of **1F**. Hence, its concentration in the dissolution medium increases up to 4 h, after which the concentration of **1F** remains constant until 22 h. This observation may be attributed to the resistance resulting from strong hydrogen bonding between CMC different chains. Consequently, water molecules need a long time to penetrate the CMC network and overcome these bonds. Besides, the poor solubility of **1F** in distilled water may increase the resistance to water penetration leading then to an increase in **1F** release which is noticed at 22 h and after water penetration to the CMC network. This causes diffusion of a small amount of the drug to the dissolution medium. The sudden decrease in **1F** release after 24 h can be probably explained by the complex formation between the positively charged **1F** and the negatively charged CMC resulting in a decrease in **1F** release. The little increase in **1F** release after 26 h may be attributed to the disintegration of the CMC network due to long contact time with the dissolution medium [26-29].

3.3.3. For CMC-2F blend

Fig. 11 shows the release dependence of **2F** from its blend with CMC. The higher release of **2F** may be due to the previously mentioned reasons for the release of **1F** where the erosion or hydration of CMC surface facilitates the liberation of **2F**, hence, its concentration in dissolution medium increases up to 4 h where it remains constant until 22 h. The difference between **2F** and **1F** may be due to the possible hydrogen bonding between the CMC matrix and the pyridine N-atom present in **1F** leading to some sort of crosslinking and consequently decrease the released amount of **1F** relative to **2F** in which N-atom is absent.

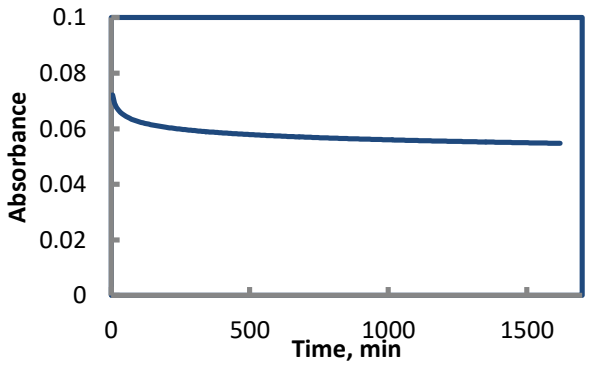

Fig. 11: Release of **2F** from CMC-**2F** blend under the room temperature and neutral pH

3.3.4. For CMC-3F blend

The behavior of the drug release for **3F** is shown in Fig. 12. Comparing the chemical structure of **3F** with both **1F** and **2F** it is obvious that **3F** contains bifuran moiety instead of bithiophene moiety in both **1F** and **2F** beside pyridine ring instead of the benzene ring in the case of **2F**. This difference in the molecular structures should be reflected more or less on the overall hydrophilic nature as well as the behavior of these compounds either from the chemical or physical point of view. Such hydrophilic nature facilitates hydrogen bonding between the bichalcophenes and the CMC matrix. It is comfortably expected that stronger hydrogen bonding would be formed in the case of **3F** with CMC rather than with **1F** or **2F** leading to more tendency of CMC-**3F** to extensively absorb more water from the dissolution medium and consequently CMC-**3F** suffers from chain scissions rupture. This leads to an increase in the swelling tendency and reduces the effective physical crosslinking formed early through the H-bonding. As an overall result, CMC-**3F** would allow the blended **3F** to be released easier and hence the release profile of **3F** from the CMC-**3F** matrix shows an increasing amount of **3F** in the dissolution medium opposite to the case for **1F** and **2F**. In all cases, the release behavior shows a gradual release of the blended bichalcophene from the CMC matrix over the processing time.

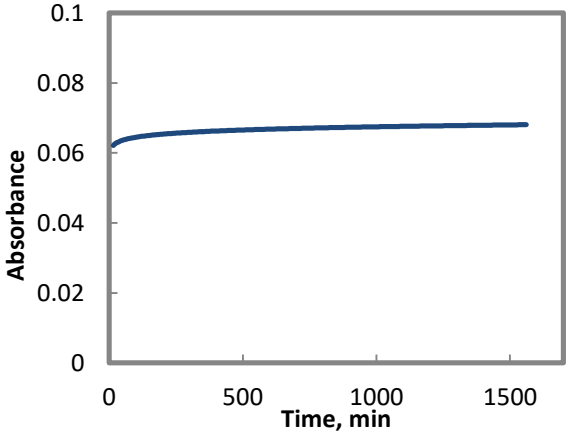

Fig. 12: Release of **3F** from CMC-**3F** blend under the room temperature and neutral pH

4. Conclusion

The results obtained in this study indicate that NaCMC has effects on the release characteristics of bichalcophene derivatives. CMC combines with positively charged active

bichalcophene derivatives producing signify-cant slower release rate. This phenomenon is attributed mainly to hydrogen bonding between anionic polymer and cationic bichalcophene derivatives, leading to a reversible polymer-drug complexation. The salt form of cationic bichalcophene derivatives show slower release rate compared to its free base that may be attributed to ionic interaction between anionic polymer and cationic derivatives. Also, the transformation of a salt form of the polymer into the acid form with low solubility in the dissolution medium prevents the diffusion of active substances through the polymer matrix leading to their release rate retardation. Solubility of the derivatives affects their release characteristics. Sparingly soluble derivatives hinder the diffusion of water molecules into the polymer matrix retarding their release rate.

4. References

1 Y. Tabata, Y. Ikada, (1998) Protein release from gelatin matrices. Adv. Drug Delivery Rev., **31**, 287–301.

2 R.A. Seigel, B.A. (1990) Firestone. Mechano-chemical to self-regulating insulin pump design. *J. Controlled Release*, **11** 181-192.

3 N.A. Peppas, R.W. Korsmeyer. (1987). Hydrogels in medicine and pharmacology. Boca Raton, FL: CRC Press

4 E.M. Al Shanqiti, K.O. Alfooty, M.Y. Abdelaal, (2021) Synthesis of chitosan nanocomposites for controlled release applications, *Int. J. Biological Macromol.*, **168** 769-774.

5 M. Kurakula, A.M. El-Helw, T.R. Sobahi, M.Y. Abdelaal, (2015) "Chitosan based atorvastatin nanocrystals: effect of cationic charge on particle size, formulation stability, and in-vivo efficacy", *Int. J. Nanomedicine*, **10** 321 – 334.

6 T.R.A. Sobahi, M.Y. Abdelaal, M.S.I. Makki, (2014) "Chemical modification of Chitosan for metal ion removal", *Arab. J. Chem.*, 7 741 – 746.

7 A.P. Rokhade, S.A. Agnihotri, S.A. Patil, N.N. Mallikarjuna, P.V. Kulkarni, T.M. (2006) Aminabhavi. Semi-interpenetrating polymer network microspheres of gelatin and sodium carboxymethylcellulose for controlled release of ketorolac tromethamine. Carbohyd. Polym., **65** 243–252.

8 M.Y. Abdelaal, T.R. Sobahi, H.F. Al-Shareef, (2013) "Modification of Chitosan derivatives of environmental and biological interest: A green chemistry approach", *Int. J. Biological Macromol.* **55** 231 – 239

9 T.R. Sobahi, M.S.I. Makki, M.Y. Abdelaal, (2013)"Carrier-Mediated blends of Chitosan with polyvinyl chloride for different applications", *J. Saudi Chem. Soc.*, **17** 245 – 250

10 M. Abdel Salam, M.S.I. Makki, M.Y. Abdelaal, (2011) "Preparation and characterization of multi-walled carbon nanotubes/chitosan nanocomposite and its application for the removal of heavy metals from aqueous solution" *J. Alloys Comp.*, **509** 2582-2587

11 T.P. Davis, M.B. Huglin. (1990) Effect of composition on properties of copolymeric N-vinyl-2pyrrolidone/methylmethacrylate hydrogels and organogels, Polymer, **31** 513-519.

12 N.P. Desai, J.A. Hubbell. (1992) Surface physical interpenetrating networks of poly(ethylene terephthalate) and poly(ethylene oxide) with biomedical applications. Macromolecules, **25** 226–232.

13 A.R. Khare, N.A. (1993) Peppas. Investigation of hydrogel water in polyelectrolyte gels using differential scanning calorimetry. Polymer, **34** 4595-4800.

14 I.M. Kenawy, M.A.H. Hafez, M.A. Ismail, M.A. Hashem. (2018) Adsorption of Cu (II), Cd (II), Hg (II), Pb (II) and Zn (II) from aqueous single metal solutions by guanyl-modified cellulose. *Int. J. Biological Macromol.*, **107** 1538-1549.

15 M.A. Hashem, M.M. Elnagar, I.M. Kenawy, M.A. (2020) Ismail. Synthesis and application of hydrazono-imidazoline modified cellulose for selective separation of precious metals from geological samples. Carbohyd. Polym. **237** 116177.

16 M.A. Taha, A.M. Dappour, M.A. Ismail, A.H. Kamel, A.A. Abdel-Shafi. (2021) Solvent polarity indicators based on

bithiophene carboxamidine hydrochloride salt derivatives. *J. Photochem. Photobiol. A: Chem.* **404** 112933.

17 H.A.Z. Sabek, A.M.M. Alazaly, D. Salah, H.S. Abdel-Samad, M.A. Ismail and A.A. Abdel-Shafi. (2020) Photophysical properties and fluorosolvatochromism of D–π–A thiophene based derivatives. RSC Adv., **10** 43459–43471.

18 A.M. Dappour, M.A. Taha, M.A. Ismail, A.A. Abdel-Shafi. (2019) Solvatochromic behavior of D-π-A bithiophene carbonitrile derivatives. *J. Mol. Liq.*, **286** 110856.

19 J.B. Hudson, L. Harris, R.J. Marles, J.T. Arnason. (1993) The anti-HIV activities of photoactive terthiophenes. Photochem. Photobiol. **58** 246-250.

20 R.J. Marles, J.B. Hudson, E.A. Graham, C. Soucy-Breau, P. Morand, R.L. Compadre, C.M. Compadre, G.H. Towers, J.T. Arnason. (1992) Structure-activity studies of photoactivated antiviral and cytotoxic tricyclic thiophenes. Photochem. Photobiol. **56** 479-487.

21 M.M. Youssef, M.A. Al-Omair, M.A. Ismail. Synthesis, DNA (2012**)** affinity, and antimicrobial activity of 4-substituted phenyl-2,2'-bichalcophenes and aza-analogues. Med. Chem. Res., **21** 4074–4082.

22 W.A. Hussin, M.A. Ismail, W.M. El-Sayed, (2013) Novel 4-substituted phenyl-2,2'-bichalcophenes and aza-analogues as antibacterial agents: A structural activity relationship, Drug Des. Devel. Ther. **7** 185-193.

23 W.M. El-Sayed, W.A. Hussin, (2013) Antimuta-genic and antioxidant activity of novel 4-substituted phenyl-2,2'-bichalcophenes and Aza-analogues, Drug Des. Devel. *Ther*. **7** 73-81.

24 M.A. Ismail, R.K. Arafa, M.M. Youssef, W.M. El-Sayed, (2014) Anticancer, antioxidant activities, and DNA affinity of novel monocationic bithiophenes and analogues. Drug Des. Devel. Ther. **8** 1659-1672.

25 W. Li, B. Sun, P. Wu. (2009) Study on hydrogen bonds of carboxymethyl cellulose sodium film with two-dimensional correlation infrared spectroscopy. Carbohyd. Polym. **78** 454–461.

26 S. Takka. (2003) Propranolol hydrochloride anionic polymer binding interaction, Il Farmaco. **58** 1051-1056.

27 D. Palmer, M. Levina, D. Douroumis, M. Maniruzzaman,D.J Morgan, T.P. Farrell, A.R. Rajabi-Siahboomi, (2013) A. Nokhodchi. Mechanism of synergistic interactions and its influence on drug release from extended release matrices manufactured using binary mixtures of polyethylene oxide and sodium carboxymethylcellulose. Colloids Surf. B: Biointerfaces **104** 174– 180.

28 C. Kim. (1998) Effects of Drug Solubility, Drug Loading, and Polymer Molecular Weight on Drug Release from Polyox Tablets. Drug Develop. Ind. Pharm. **24** 645-651.

29 A.S. Hussain**,** R.D. Johnson, P. Shivanand, M.A. Zoglio. (1994) Effects of blending a nonionic and an anionic cellulose ether polymer on drug release from hydrophilic matrix capsules. Drug Develop. Ind. Pharm. **20** 2645-2657.